World Journal of Radiology

Online Submissions: http://www.wjgnet.com/1949-8470office
wjr@wjgnet.com
doi:10.4329/wjr.v2.i5.180

World J Radiol 2010 May 28; 2(5): 180-187
ISSN 1949-8470 (online)

REVIEW

Multi-parametric MR imaging of transition zone prostate cancer: Imaging features, detection and staging

Arda Kayhan, Xiaobing Fan, Jacob Oommen, Aytekin Oto

Arda Kayhan, Xiaobing Fan, Jacob Oommen, Aytekin Oto, Department of Radiology, University of Chicago, Chicago, IL 60637, United States

Author contributions: Kayhan A wrote the article; Fan X organized the references and drafted the article; Oommen J collected and assembled the data; Oto A revised the article.

Correspondence to: Arda Kayhan, MD, Department of Radiology, University of Chicago, Chicago, IL, United States. arda_kayhan@yahoo.com

Telephone: +1-773-7021310 Fax: +1-773-8347448

Received: March 30, 2010 Revised: April 21, 2010
Accepted: April 28, 2010
Published online: May 28, 2010

Abstract

Magnetic resonance (MR) imaging has been increasingly used in the evaluation of prostate cancer. As studies have suggested that the majority of cancers arise from the peripheral zone (PZ), MR imaging has focused on the PZ of the prostate gland thus far. However, a considerable number of cancers (up to 30%) originate in the transition zone (TZ), substantially contributing to morbidity and mortality. Therefore, research is needed on the TZ of the prostate gland. Recently, MR imaging and advanced MR techniques have been gaining acceptance in evaluation of the TZ. In this article, the MR imaging features of TZ prostate cancers, the role of MR imaging in TZ cancer detection and staging, and recent advanced MR techniques will be discussed in light of the literature.

Key words: Multi-parametric magnetic resonance imaging; Prostate cancer; Transition zone

Peer reviewers: James Chow, PhD, Radiation Physicist, Radiation Medicine Program, Princess Margaret Hospital, 610 University Avenue, Toronto, ON, M5G 2M9, Canada; Chan Kyo Kim, MD, Assistant Professor, Department of Radiology, Samsung Medical Center, Sungkyunkwan University School of Medicine, 50 Ilwon-dong, Kangnam-gu, Seoul 135-710, South Korea

Kayhan A, Fan X, Oommen J, Oto A. Multi-parametric MR imaging of transition zone prostate cancer: Imaging features, detection and staging. *World J Radiol* 2010; 2(5): 180-187 Available from: URL: http://www.wjgnet.com/1949-8470/full/v2/i5/180.htm DOI: http://dx.doi.org/10.4329/wjr.v2.i5.180

INTRODUCTION

It is important to localize prostate gland tumors to evaluate the transcapsular spread and staging in order to plan treatment protocols and avoid positive anterior surgical margins during radical prostatectomy. Prostate cancer arises from the peripheral zone (PZ) in 75%-85% of patients[1]. Cancers arising from the transition zone (TZ) represent 40% of autopsy series and 25%-30% of radical prostatectomy series[1]. The utility of magnetic resonance (MR) imaging in prostate cancer is currently under investigation, and it has been shown to be an excellent technique for evaluating prostate cancers, particularly PZ cancers[2,3]. As TZ cancers are less frequent than PZ cancers, MR imaging in TZ cancers has not been widely used. However, recent studies attempting to identify MR characteristics of the TZ, by means of emerging techniques, have shown that MR can be used to delineate TZ cancers accurately[4-7]. Herein, the MR imaging features of TZ tumors, the role of MR imaging in detection and staging, and recent advanced MR techniques in the evaluation of TZ cancers will be discussed including a review of literature.

ANATOMY AND MR IMAGING OF THE PROSTATE GLAND

According to zonal anatomy, the prostate is composed of anterior fibromuscular stroma, periurethral glandular

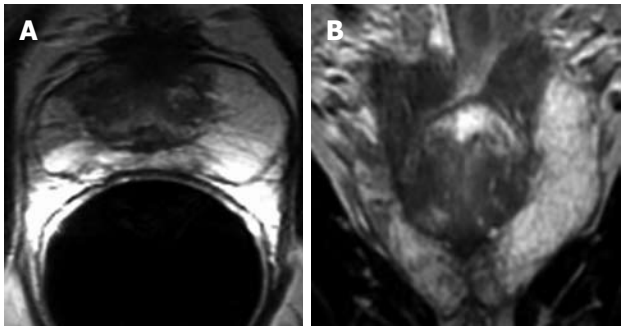

Figure 1 Magnetic resonance (MR) images demonstrating zonal anatomy of prostate gland. A: Axial T2-weighted (T2W) MR image depicts the central gland and peripheral zone (PZ). Central gland is hypointense compared to hyperintense PZ; B. Coronal T2W MR image shows hyperintense PZ and hypointense central gland.

tissue, the TZ, central zone (CZ) and PZ. The TZ is the inner prostate and forms 5% of the gland. It surrounds the anterior and lateral parts of the proximal urethra. In younger men this zone is small, however, with aging it enlarges and compresses the CZ due to hyperplastic changes. The CZ is the outer prostate forming approximately 25% of the gland in young men[8]. It is less clearly distinguished histologically from the PZ. The PZ is the outer prostate and forms 70% of the gland[8]. Radiologically, the prostate has been divided into two parts: the PZ and the central gland which is composed of the PZ, TZ and CZ[9]. In young men, the gland is mainly composed of the CZ. With aging, the TZ is enlarged due to benign prostatic hyperplasia (BPH) which commonly arises from the TZ[10].

MR imaging enables differentiation between the PZ, CZ and TZ. In young adults, normal prostate is homogenous, whereas with aging the differentiation between the PZ and the central gland is more clearly depicted. T1-weighted (T1W) images distinguish between the prostatic parenchyma and the surrounding periprostatic fat and vascular plexus. On T1W images, the homogenous gland has an intermediate-to-low signal intensity, and zonal differentiation can not be identified[11]. Post-biopsy hemorrhage has high signal-intensity on T1W images. On T2-weighted (T2W) images, better tissue differentiation is achieved and zonal anatomy is better depicted[12]. As the glandular components are more prominent in the PZ, it has a homogeneously high signal intensity and is surrounded by a capsule which is seen as a thin, hypointense rim on T2W images. Both the CZ and TZ are hypointense compared to the PZ because of their stroma which consists of compact muscle fiber bundles. MR also enables multiplanar imaging of the prostate (Figure 1).

MR imaging has been increasingly used in the evaluation of prostate cancer[13-18]. It enables multiplanar imaging and is superior to ultrasound and computed tomography in anatomic and volumetric evaluation of the gland[19]. It is more accurate than digital rectal examination and transrectal ultrasound (TRUS)-guided biopsy for cancer detection and localization. In a recent study, the detectability of prostate cancer using MR imaging prior to TRUS-guided biopsy was determined by calculating the sensitivity and positive predictive value of TRUS, T2W imaging, diffusion weighted imaging (DWI), apparent diffusion coefficient (ADC) map and biopsy[20]. The relationship between the detectability on each sequence and cancer location, Gleason score, and the short and long axis diameter of the tumor were also evaluated. The sensitivities were 26.9%, 41.2%, 56.7%, 57.7% and 75.1%, respectively. The sensitivity of each sequence increased as the Gleason score and the short- and long-axis diameters of the tumors increased. It was stated that MR imaging prior to biopsy has a high detectability for prostate cancer. MR imaging is used to guide targeted biopsy when prostate cancer is clinically suspected and previous ultrasound-guided biopsy results are negative. MR imaging also enables the localization and staging of prostate cancer. The high soft tissue resolution of MR imaging helps to show extracapsular extension and seminal vesicle invasion. It may be used in planning a roadmap for therapeutic approaches and for residual or locally recurrent cancer after treatment. MR imaging has mainly been used as a diagnostic tool for the detection of PZ cancers[18-21]. It is considered insufficient for evaluating the TZ, as BPH, which causes a heterogenous signal intensity, especially in elderly men, also originates from the TZ leading to conspicuous findings on T2W images[2,22,23]. Recent studies using MR imaging of TZ cancers have shown that it can be used in the detection of TZ tumors that are not sampled during TRUS-guided biopsy and also for localization and staging[4].

MR IMAGING OF TZ CANCERS

Prostate cancer begins as a small focus of carcinoma within the gland which grows very slowly[24]. Approximately 75%-85% of cancers arise from the PZ, 25% arise from the TZ and 10% arise from the CZ[1,25,26]. As there is no clear demarcation between the CZ and the PZ, most pathologists do not routinely recognize tumors as originating from the CZ. For that reason, comparison is generally focused on the distinctions between PZ and TZ cancers. TZ tumors are located anteriorly, far from the rectum and they are more difficult to detect compared to PZ tumors. These tumors can be of a large volume and are associated with high serum prostate specific antigen (PSA) levels but they are confined to the gland[27]. They are mostly low grade and relatively non-aggressive. Most TZ tumors are found incidentally in resection specimens. It is important to accurately distinguish TZ cancers to guide biopsy and to avoid positive anterior surgical margins at radical prostatectomy.

Currently, the PZ is the primary target in most biopsies[28]. However, in patients with elevated PSA levels with negative biopsy results, it should be kept in mind that the tumor focus may be in the central gland. Therefore, it has been suggested that TZ-targeted biopsy should be performed in patients with multiple negative biopsy results. As a result, although tumor zonal origin is

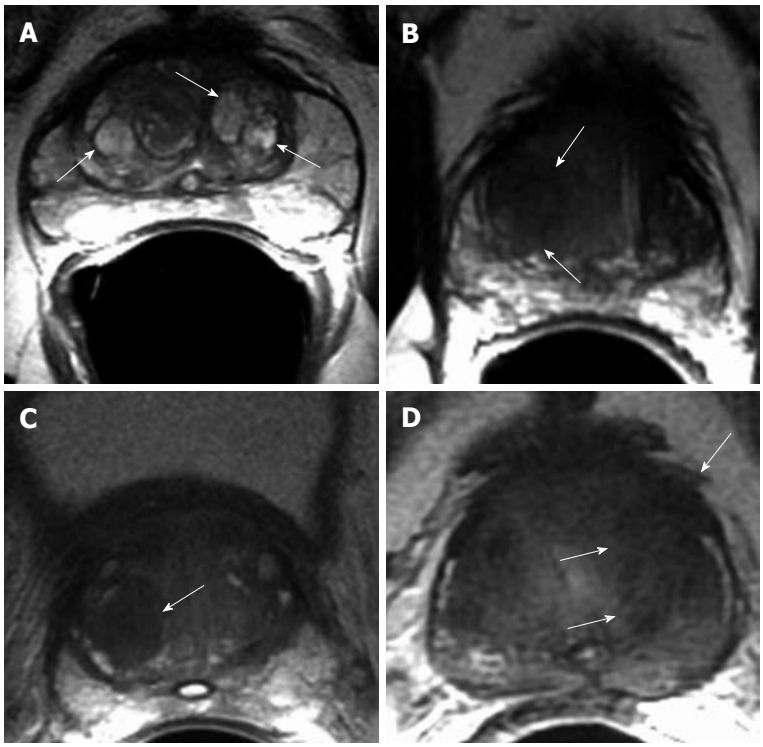

Figure 2 Axial T2W MR image. A: Multiple, well defined hyperintense glandular benign prostatic hyperplasia (BPH) nodules in central gland (arrows); B: Well defined, amorphous, hypointense TZ tumor (arrows); C: Hypointense stromal BPH nodule in the right transition zone (TZ) (arrow); D: Hypointense TZ tumor with extracapsular extension (arrows).

not an independent determinant of biochemical failure, it is helpful in predicting the route of cancer spread. If the zonal origin can be determined preoperatively, the cure rate may be increased by modification of the surgical approach.

The central gland has a heterogeneously variable signal intensity appearance in older men due to the presence of BPH or other coexisting benign diseases. BPH nodules occur almost exclusively in the TZ. As hypertrophied TZ tissue might also show metabolic heterogeneity similar to BPH nodules, it may be difficult to differentiate them from carcinoma. Discrimination between BPH and central gland tumors is important for staging. BPH is an enlargement of the TZ (central gland) which gives a heterogeneous appearance on MR imaging[29,30]. BPH nodules may be seen as hypointense, isointense or hyperintense on T2W images, depending on the ratio of glandular to stromal tissue[31]. It has been shown that, high signal intensity is due to hyperplastic glandular elements which are filled with secretion and the presence of cystic ectasia (Figure 2A). Low signal intensity is due to the presence of prominent sclerotic, fibrous or muscular elements[22,29] (Figure 2B).

TZ cancers tend to have uniform low intensity on T2W imaging, but their diagnosis is not certain in the presence of coexisting benign disease[31,32] (Figure 2C and D). It has been shown that, unless cancers in the TZ are of a large dimension, their detection on MR imaging is very difficult[33]. Akin *et al*[4] determined the accuracy of MR imaging in detection and local staging in 148 patients. Features indicative of TZ cancers were defined as: homogenous low T2 signal intensity, ill defined margins, lack of capsule, lenticular shape, and invasion of anterior fibromuscular stroma. For identification of patients with TZ cancer, the sensitivity of MR imaging was 75%-80% and the specificity was 78%-87%. The area under the receiver operating characteristic curve was 0.75 for detection and localization of tumor. For detection of extraprostatic extension, the sensitivity and specificity of MR imaging were 28%-56% and 93%-94%, respectively. Li *et al*[5] determined the conventional MR findings of TZ lesions in 86 patients, of which 53 were cancers and 33 were benign, by comparing T2W and contrast-enhanced T1W images. Lesions were classified as uniform, low signal intensity on T2W images, lesions with homogeneous contrast enhancement and lesions with irregular margins on both gadolinium enhanced T1 and T2W images. Sensitivity, specificity and accuracy for cancer were 50%, 51% and 51%, respectively, for the uniform low T2 signal intensity criterion; 68%, 75% and 71% for homogeneous gadolinium enhancement; 60%, 72% and 65% for irregular margins on both T2W and gadolinium enhanced images.

ADVANCED MR TECHNIQUES

TZ cancers are difficult to diagnose particularly in the presence of BPH. Even in the PZ, some cancers such as those with a more permeative pattern can not be detected. Moreover, focal prostatic atrophy or prostatitis may also mimic cancer and may cause false-positive results. To increase the accuracy of MR imaging and to improve the detection of prostate cancer at an earlier stage, special techniques such as DWI, dynamic contrast-enhanced MR imaging (DCE-MRI), MR spectroscopy (MRS) and high-field-strength (3.0-T) MR imaging have been increasingly used. It has also been shown that these techniques may play a role in the detection of prostate tumor

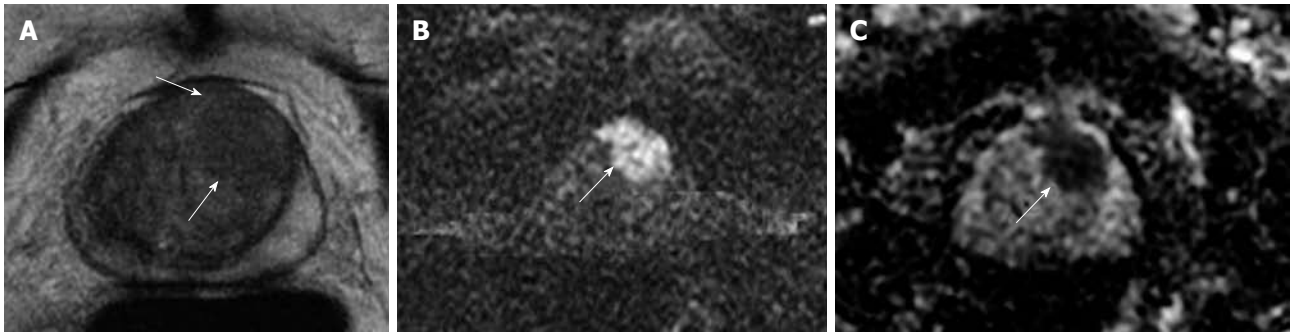

Figure 3 Tumor in the left mid prostate gland demonstrated by MR. A: Axial T2W image shows ill defined, amorphous, hypointense tumor (arrows); B: Diffusion weighted imaging (DWI) reveals focal area of bright signal consistent with tumor(arrow); C: Apparent diffusion coefficient (ADC) map reveals clear focal mass with dark signal consistent with decreased ADC (arrow).

foci in patients with persistently elevated PSA levels and prior to negative random TRUS-guided biopsy[34].

DWI

DWI is a technique sensitive to molecular translation of water in biologic tissues due to the random thermal motion of molecules. The rapid changes in the movement of water in tissues and the measurement of the flow of water molecules can be identified by calculating the ADC[35]. When the flow of water or diffusion is restricted, ADC is decreased. If ADC values are increased, there is no restriction in water flow. The ADC has been determined for tumor growth. It has been shown that, in proliferating cells, cellular density increases and extra- as well as intracellular space decreases leading to decreased ADC[36]. In recent years, an increased number of studies have evaluated the utility of DWI in prostate cancer diagnosis[37-44]. It has been shown that cancer tissues show higher signal intensity on DWI and thus a lower ADC compared with BPH nodules and normal tissue due to replacement of normal tissue (composed of water rich acinar structures) with densely packed malignant epithelial cells. TZ tumors have also been shown to have lower ADC values than the surrounding tissue[37] (Figure 3). Namiki *et al*[45] stated that different b factors may effect the detection of tumors. Noworolski *et al*[41] showed that glandular-ductal tissues (glandular BPH) had lower peak enhancement and higher ADC values than the stromal-low ductal tissues (stromal BPH and central gland). Oto *et al*[46] showed significant ADC differences between tumor, stromal BPH and glandular BPH (lowest in tumor, highest in glandular BPH). These authors stated that there were differences between the perfusion parameters of tumor, stromal and glandular BPH, with the exception of the k-trans values between tumor and glandular BPH. Tamada *et al*[47] compared the ADC values in peripheral and transitional zones between normal and malignant prostatic tissues. Mean ADC values were significantly lower in both the PZ and TZ than in the corresponding normal regions. Ren *et al*[48] investigated the diagnostic value of DWI and ADC values in normal and pathologic prostate tissues. They showed that BPH nodules had a lower and non-homogenous signal intensity than the PZ. Prostate cancer showed high signal intensity while prostate cyst showed low intensity. ADC values of BPH nodules were larger than prostate cancer foci and normal central gland. They stated that DWI and ADC values for normal central gland, PZ, prostate cyst, BPH nodules and cancer foci showed significant differences and could be used in the differential diagnosis of diseases of the prostate gland. Yoshizako *et al*[6] determined the clinical value of DWI and DCE-MRI in combination with T2W images, for the diagnosis of TZ tumors. They found that adding DWI to T2W images improved the sensitivity, specificity, accuracy and positive predictive value of diagnosing TZ tumors. In a recent study, the need for biexponential signal decay modeling for prostate cancer diffusion signal decays with b-factor over an extended b-factor range was evaluated. The researchers found that the fast and slow ADC values of cancer were significantly lower than those of the TZ and PZ, and the apparent fraction of the fast diffusion component was significantly smaller in cancer than in the PZ. It was stated that biexponential diffusion decay functions were required for prostate cancer diffusion signal decay curves when sampled over an extended b-factor range, enabling specific tissue characterization of prostate cancers[49].

DCE-MRI

DCE-MRI was introduced to effectively visualize the pharmacokinetics of gadolinium uptake in the prostate gland. It depicts the physiological function of the tumor microcirculation. There is a relationship between contrast material uptake and microvascular structures in tumors, in which tumor angiogenesis is correlated with the parameters of signal intensity-time curves. As the reliability of T2W MR imaging in distinguishing prostate cancer of the PZ and TZ is limited, several studies have been performed to delineate the enhancement characteristics of prostate cancer to achieve more accurate information[2,50-53]. In a recent study, the accuracy of T2W and DCE-MRI for cancer detection in 18 prostate cancer patients were compared prior to prostatectomy[54]. The accuracy of DCE-MRI for cancer detection was calculated by a pixel-by-pixel correlation of quantitative DCE-MRI parameter maps and pathology. It was shown that DCE-MRI was more sensitive than T2W images for

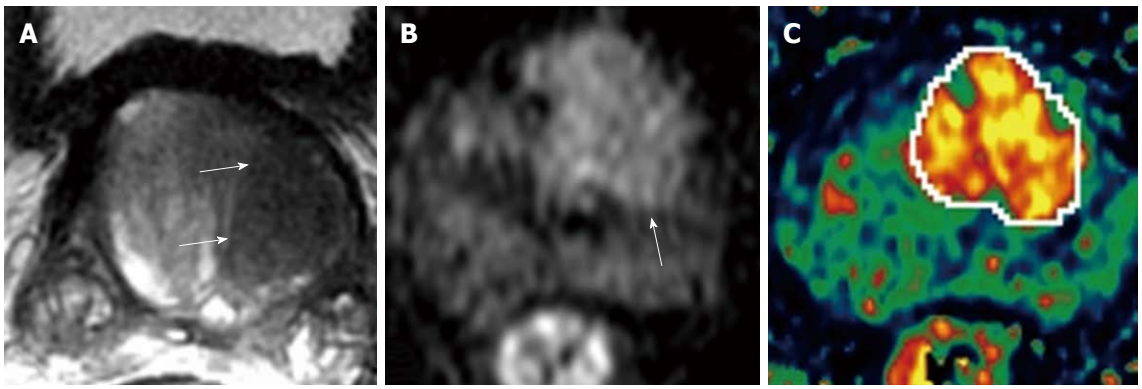

Figure 4 Left TZ tumor of prostate gland demonstrated by MR. A: Axial T2W image depicts ill defined, round, homogenous hypointense tumor (arrows); B: DWI depicts focal area of bright signal on left mid gland (arrow); C: K-trans map in dynamic contrast-enhanced MR imaging (DCE-MRI) clearly localizes the tumor and reveals some internal heterogeneity.

tumor localization (50% *vs* 21%) and more specific (85% *vs* 81%). The researchers stated that due to its higher sensitivity and specificity, DCE-MRI could be used to guide radiotherapy boosts in prostate cancer patients. Due to increased microvessel density (MVD) in carcinomatous tissue, the enhancement curve of prostate tumors was shown to be different when compared to the PZ and BPH. Engelbrecht *et al*[55] found that in both the PZ and TZ, the relative peak enhancement was the optimal parameter when compared to other parameters such as onset time, time to peak, peak enhancement and wash-out. Yoshizako *et al*[6] stated that the addition of DCE-MRI to T2W images and DWI improved the specificity and positive predictive value of diagnosing TZ cancer (93.8% and 94.7%, respectively). Turnbull *et al*[2] found significant differences in amplitude of the initial enhancement and wash-out patterns between carcinoma and BPH. In both the PZ and the central gland, relative peak enhancement was the optimal parameter. The combination of relative peak enhancement with other dynamic parameters (onset time, time to peak, peak enhancement, and washout) did not yield a significant gain in discriminatory performance. Ogura *et al*[56] demonstrated a sensitivity, specificity and accuracy rate of 37%, 97% and 63%, respectively, for the detection of TZ cancer. In another study, it was shown that the glandular-ductal tissues had lower peak enhancement than the stromal-low ductal tissues suggesting that gadolinium-DTPA does not enter healthy prostatic tissues[2]. Ren *et al*[57] examined DCE-MRI parameters in 21 patients with prostate cancer and 29 patients with BPH by means of signal intensity-time curves and angiogenesis. Prostate cancer showed stronger enhancement with an earlier peak time, higher enhancement and enhancement rate. The vascular endothelial growth factor (VEGF) and MVD expression levels in cancer were higher than in BPH. They found a negative correlation between peak time and the expression levels of VEGF and MVD, however, the degree of enhancement and enhancement rate showed positive correlations.

In cancerous tissues, there is uncontrolled angiogenesis and the permeability of vascular structures is markedly increased resulting in significantly different pharmacokinetics compared to surrounding normal tissue. Pharmacokinetic parameter mapping clearly identifies pathologic areas in heterogeneously enhanced prostate. K-trans maps enable the identification of tumor within heterogeneously enhanced PZ and can reveal the extent of extra-glandular involvement. These maps may also be useful in providing a biopsy target and in revealing intra-tumoral heterogeneity (Figure 4).

MRS

MRS imaging is an emerging technique used in combination with MRI in the evaluation of prostate cancer[58-63]. This technique allows the metabolites within tissues to be identified and provides information on the biochemical and metabolic environment of tissues. As prostate is composed of different types of glands and tissues, it is difficult to study the gland using MRS. However; there are sophisticated chemical shift filtering techniques and three dimensional chemical shift imaging which allow examination of the entire prostate at one time and the selection of particular chemicals for diagnosis[59,64]. It has been shown that stromal and glandular tissue have the same resonances with different relative peak height intensities[65]. In addition, it has been stated that citrate is produced by glandular epithelial cells and the amount of glandular elements can affect tissue citrate levels. Glandular BPH has higher levels of citrate than stromal BPH[66]. It has also been stated that citrate levels show the degree of tissue differentiation, in that poorly differentiated tumors have lower citrate levels than well differentiated tumors[67]. Healthy PZ is known to have high citrate content, whereas in cancer tissues, the resonance signal from citrate is reduced or even absent. Adenocarcinomatous tissue in the prostate gland also shows a similar spectrum to adenocarcinoma in other organs (except for citrate)[68], which show elevated choline relative to creatine due to the increased cell proliferation associated with malignant tumors[69]. In their series performed in 40 patients, Zakian *et al*[7] studied the mean values of choline + creatine/citrate, choline/creatine and choline/citrate in TZ cancer

and normal tissue, in which a significant difference was found. It was shown that 56% of patients had tumor voxels with at least one detectable choline peak, while control voxels showed only choline peaks.

3.0-T MR imaging

High-field-strength MR imaging has recently been investigated in prostate imaging. The introduction of 3.0-T MR scanners has resulted in an increase in the in-plane resolution of anatomic T2W imaging due to higher signal to noise ratio. Higher magnetic field strengths have been shown to enable structural imaging of the prostate with improved spatial resolution leading to improved detection and staging of PZ tumors[70-72]. Moreover, functional imaging such as DWI, DCE-MRI or MRS at high field strength is thought to improve the detection of CZ and TZ cancers, prevent false-positive diagnoses and help less experienced readers to improve their local staging performance[73,74].

CONCLUSION

TZ cancers demonstrate similar imaging features to BPH and are therefore more difficult to diagnose on MR imaging. However, certain imaging features (alone or in combination) on multi-parametric MR imaging can help in the differentiation between cancerous and benign TZ tissue. MR imaging can also provide reliable local staging of TZ cancers. By the addition of emerging MR techniques, such as DWI, DCE-MRI, MRS and high-field-strength (3.0-T) MR imaging to standard T2W images, MR imaging has now become a promising technique in the evaluation of TZ tumors.

REFERENCES

1 **McNeal JE**, Redwine EA, Freiha FS, Stamey TA. Zonal distribution of prostatic adenocarcinoma. Correlation with histologic pattern and direction of spread. *Am J Surg Pathol* 1988; **12**: 897-906
2 **Turnbull LW**, Buckley DL, Turnbull LS, Liney GP, Knowles AJ. Differentiation of prostatic carcinoma and benign prostatic hyperplasia: correlation between dynamic Gd-DTPA-enhanced MR imaging and histopathology. *J Magn Reson Imaging* 1999; **9**: 311-316
3 **Tamada T**, Sone T, Nagai K, Jo Y, Gyoten M, Imai S, Kajihara Y, Fukunaga M. T2-weighted MR imaging of prostate cancer: multishot echo-planar imaging vs fast spin-echo imaging. *Eur Radiol* 2004; **14**: 318-325
4 **Akin O**, Sala E, Moskowitz CS, Kuroiwa K, Ishill NM, Pucar D, Scardino PT, Hricak H. Transition zone prostate cancers: features, detection, localization, and staging at endorectal MR imaging. *Radiology* 2006; **239**: 784-792
5 **Li H**, Sugimura K, Kaji Y, Kitamura Y, Fujii M, Hara I, Tachibana M. Conventional MRI capabilities in the diagnosis of prostate cancer in the transition zone. *AJR Am J Roentgenol* 2006; **186**: 729-742
6 **Yoshizako T**, Wada A, Hayashi T, Uchida K, Sumura M, Uchida N, Kitagaki H, Igawa M. Usefulness of diffusion-weighted imaging and dynamic contrast-enhanced magnetic resonance imaging in the diagnosis of prostate transition-zone cancer. *Acta Radiol* 2008; **49**: 1207-1213
7 **Zakian KL**, Eberhardt S, Hricak H, Shukla-Dave A, Kleinman S, Muruganandham M, Sircar K, Kattan MW, Reuter VE, Scardino PT, Koutcher JA. Transition zone prostate cancer: metabolic characteristics at 1H MR spectroscopic imaging--initial results. *Radiology* 2003; **229**: 241-247
8 **Stamey TA**, McNeal JE. Adenocarcinoma of the prostate. In: Walsh PC, Retik AB, Stamey TA, Vaughan ED, editors. Campbell's Urology. 6th ed. Philedelphia: WB Saunders, 1992: 643-658
9 **Older RA**, Watson LR. Ultrasound anatomy of the normal male reproductive tract. *J Clin Ultrasound* 1996; **24**: 389-404
10 **De Marzo AM**, Coffey DS, Nelson WG. New concepts in tissue specificity for prostate cancer and benign prostatic hyperplasia. *Urology* 1999; **53**: 29-39; discussion 39-42
11 **Hricak H**. The prostate gland. In: Hricak H, Carrington B, editors. MRI of the pelvis. London: Martin Dunitz, 1991: 249-311
12 **McNeal JE**. The prostate gland: morphology and pathology. *Monogr Urol* 1983: **4**: 5-13
13 **Engelbrecht MR**, Jager GJ, Laheij RJ, Verbeek AL, van Lier HJ, Barentsz JO. Local staging of prostate cancer using magnetic resonance imaging: a meta-analysis. *Eur Radiol* 2002; **12**: 2294-2302
14 **Jager GJ**, Ruijter ET, van de Kaa CA, de la Rosette JJ, Oosterhof GO, Thornbury JR, Barentsz JO. Local staging of prostate cancer with endorectal MR imaging: correlation with histopathology. *AJR Am J Roentgenol* 1996; **166**: 845-852
15 **Cornud F**, Hamida K, Flam T, Hélénon O, Chrétien Y, Thiounn N, Correas JM, Casanova JM, Moreau JF. Endorectal color doppler sonography and endorectal MR imaging features of nonpalpable prostate cancer: correlation with radical prostatectomy findings. *AJR Am J Roentgenol* 2000; **175**: 1161-1168
16 **Cornud F**, Flam T, Chauveinc L, Hamida K, Chrétien Y, Vieillefond A, Hélénon O, Moreau JF. Extraprostatic spread of clinically localized prostate cancer: factors predictive of pT3 tumor and of positive endorectal MR imaging examination results. *Radiology* 2002; **224**: 203-210
17 **Soulié M**, Aziza R, Escourrou G, Seguin P, Tollon C, Molinier L, Bachaud J, Joffre F, Plante P. Assessment of the risk of positive surgical margins with pelvic phased-array magnetic resonance imaging in patients with clinically localized prostate cancer: a prospective study. *Urology* 2001; **58**: 228-232
18 **Cruz M**, Tsuda K, Narumi Y, Kuroiwa Y, Nose T, Kojima Y, Okuyama A, Takahashi S, Aozasa K, Barentsz JO, Nakamura H. Characterization of low-intensity lesions in the peripheral zone of prostate on pre-biopsy endorectal coil MR imaging. *Eur Radiol* 2002; **12**: 357-365
19 **Hricak H**, Williams RD, Spring DB, Moon KL Jr, Hedgcock MW, Watson RA, Crooks LE. Anatomy and pathology of the male pelvis by magnetic resonance imaging. *AJR Am J Roentgenol* 1983; **141**: 1101-1110
20 **Shimizu T**, Nishie A, Ro T, Tajima T, Yamaguchi A, Kono S, Honda H. Prostate cancer detection: the value of performing an MRI before a biopsy. *Acta Radiol* 2009; **50**: 1080-1088
21 **Claus FG**, Hricak H, Hattery RR. Pretreatment evaluation of prostate cancer: role of MR imaging and 1H MR spectroscopy. *Radiographics* 2004; **24** Suppl 1: S167-S180
22 **Schiebler ML**, Tomaszewski JE, Bezzi M, Pollack HM, Kressel HY, Cohen EK, Altman HG, Gefter WB, Wein AJ, Axel L. Prostatic carcinoma and benign prostatic hyperplasia: correlation of high-resolution MR and histopathologic findings. *Radiology* 1989; **172**: 131-137
23 **Muramoto S**, Uematsu H, Kimura H, Ishimori Y, Sadato N, Oyama N, Matsuda T, Kawamura Y, Yonekura Y, Okada K, Itoh H. Differentiation of prostate cancer from benign prostate hypertrophy using dual-echo dynamic contrast MR imaging. *Eur J Radiol* 2002; **44**: 52-58
24 **McNeal JE**, Bostwick DG, Kindrachuk RA, Redwine EA, Freiha FS, Stamey TA. Patterns of progression in prostate cancer. *Lancet* 1986; **1**: 60-63
25 **Stamey TA**, Donaldson AN, Yemoto CE, McNeal JE, Sözen S, Gill H. Histological and clinical findings in 896 consecutive prostates treated only with radical retropubic prostatec-

tomy: epidemiologic significance of annual changes. *J Urol* 1998; **160**: 2412-2417
26 **Augustin H**, Erbersdobler A, Graefen M, Fernandez S, Palisaar J, Huland H, Hammerer P. Biochemical recurrence following radical prostatectomy: a comparison between prostate cancers located in different anatomical zones. *Prostate* 2003; **55**: 48-54
27 **Pavelić J**, Zeljko Z, Bosnar MH. Molecular genetic aspects of prostate transition zone lesions. *Urology* 2003; **62**: 607-613
28 **Liu IJ**, Macy M, Lai YH, Terris MK. Critical evaluation of the current indications for transition zone biopsies. *Urology* 2001; **57**: 1117-1120
29 **Pollack HM**. Imaging of the prostate gland. *Eur Urol* 1991; **20** Suppl 1: 50-58
30 **Grossfeld GD**, Coakley FV. Benign prostatic hyperplasia: clinical overview and value of diagnostic imaging. *Radiol Clin North Am* 2000; **38**: 31-47
31 **Ling D**, Lee JK, Heiken JP, Balfe DM, Glazer HS, McClennan BL. Prostatic carcinoma and benign prostatic hyperplasia: inability of MR imaging to distinguish between the two diseases. *Radiology* 1986; **158**: 103-107
32 **Poon PY**, McCallum RW, Henkelman MM, Bronskill MJ, Sutcliffe SB, Jewett MA, Rider WD, Bruce AW. Magnetic resonance imaging of the prostate. *Radiology* 1985; **154**: 143-149
33 **Ellis JH**, Tempany C, Sarin MS, Gatsonis C, Rifkin MD, McNeil BJ. MR imaging and sonography of early prostatic cancer: pathologic and imaging features that influence identification and diagnosis. *AJR Am J Roentgenol* 1994; **162**: 865-872
34 **Sciarra A**, Panebianco V, Ciccariello M, Salciccia S, Cattarino S, Lisi D, Gentilucci A, Alfarone A, Bernardo S, Passariello R, Gentile V. Value of magnetic resonance spectroscopy imaging and dynamic contrast-enhanced imaging for detecting prostate cancer foci in men with prior negative biopsy. *Clin Cancer Res* 2010; **16**: 1875-1883
35 **Bammer R**. Basic principles of diffusion-weighted imaging. *Eur J Radiol* 2003; **45**: 169-184
36 **Chenevert TL**, Stegman LD, Taylor JM, Robertson PL, Greenberg HS, Rehemtulla A, Ross BD. Diffusion magnetic resonance imaging: an early surrogate marker of therapeutic efficacy in brain tumors. *J Natl Cancer Inst* 2000; **92**: 2029-2036
37 **Sato C**, Naganawa S, Nakamura T, Kumada H, Miura S, Takizawa O, Ishigaki T. Differentiation of noncancerous tissue and cancer lesions by apparent diffusion coefficient values in transition and peripheral zones of the prostate. *J Magn Reson Imaging* 2005; **21**: 258-262
38 **Kozlowski P**, Chang SD, Jones EC, Berean KW, Chen H, Goldenberg SL. Combined diffusion-weighted and dynamic contrast-enhanced MRI for prostate cancer diagnosis--correlation with biopsy and histopathology. *J Magn Reson Imaging* 2006; **24**: 108-113
39 **Tanimoto A**, Nakashima J, Kohno H, Shinmoto H, Kuribayashi S. Prostate cancer screening: the clinical value of diffusion-weighted imaging and dynamic MR imaging in combination with T2-weighted imaging. *J Magn Reson Imaging* 2007; **25**: 146-152
40 **desouza NM**, Reinsberg SA, Scurr ED, Brewster JM, Payne GS. Magnetic resonance imaging in prostate cancer: the value of apparent diffusion coefficients for identifying malignant nodules. *Br J Radiol* 2007; **80**: 90-95
41 **Noworolski SM**, Vigneron DB, Chen AP, Kurhanewicz J. Dynamic contrast-enhanced MRI and MR diffusion imaging to distinguish between glandular and stromal prostatic tissues. *Magn Reson Imaging* 2008; **26**: 1071-1080
42 **Kim JH**, Kim JK, Park BW, Kim N, Cho KS. Apparent diffusion coefficient: prostate cancer versus noncancerous tissue according to anatomical region. *J Magn Reson Imaging* 2008; **28**: 1173-1179
43 **Reinsberg SA**, Payne GS, Riches SF, Ashley S, Brewster JM, Morgan VA, deSouza NM. Combined use of diffusion-weighted MRI and 1H MR spectroscopy to increase accuracy in prostate cancer detection. *AJR Am J Roentgenol* 2007; **188**: 91-98
44 **Yoshimitsu K**, Kiyoshima K, Irie H, Tajima T, Asayama Y, Hirakawa M, Ishigami K, Naito S, Honda H. Usefulness of apparent diffusion coefficient map in diagnosing prostate carcinoma: correlation with stepwise histopathology. *J Magn Reson Imaging* 2008; **27**: 132-139
45 **Namiki T**, Koyama K, Tanaka H, Ohmura M, Harada J, Fukuda K. Effect of diffusion-weighted imaging with very high b-factors for detection of prostate cancer. In: Proceedings of the Radiological Society of North America annual meeting. Chicago, 2005: 649
46 **Oto A**, Kayhan A, Tretiakova M, Yang C, Jiang Y, Stadler WM. Role of DWI and DCE-MRI to Distinguish Transitional Zone Prostate Cancer from Benign Prostatic Hyperplasia. In: Proceedings of the Radiologic Society of North America annual meeting. Chicago, 2009
47 **Tamada T**, Sone T, Jo Y, Toshimitsu S, Yamashita T, Yamamoto A, Tanimoto D, Ito K. Apparent diffusion coefficient values in peripheral and transition zones of the prostate: comparison between normal and malignant prostatic tissues and correlation with histologic grade. *J Magn Reson Imaging* 2008; **28**: 720-726
48 **Ren J**, Huan Y, Wang H, Zhao H, Ge Y, Chang Y, Liu Y. Diffusion-weighted imaging in normal prostate and differential diagnosis of prostate diseases. *Abdom Imaging* 2008; **33**: 724-728
49 **Shinmoto H**, Oshio K, Tanimoto A, Higuchi N, Okuda S, Kuribayashi S, Mulkern RV. Biexponential apparent diffusion coefficients in prostate cancer. *Magn Reson Imaging* 2009; **27**: 355-359
50 **Preziosi P**, Orlacchio A, Di Giambattista G, Di Renzi P, Bortolotti L, Fabiano A, Cruciani E, Pasqualetti P. Enhancement patterns of prostate cancer in dynamic MRI. *Eur Radiol* 2003; **13**: 925-930
51 **Rouvière O**, Raudrant A, Ecochard R, Colin-Pangaud C, Pasquiou C, Bouvier R, Maréchal JM, Lyonnet D. Characterization of time-enhancement curves of benign and malignant prostate tissue at dynamic MR imaging. *Eur Radiol* 2003; **13**: 931-942
52 **Hara N**, Okuizumi M, Koike H, Kawaguchi M, Bilim V. Dynamic contrast-enhanced magnetic resonance imaging (DCE-MRI) is a useful modality for the precise detection and staging of early prostate cancer. *Prostate* 2005; **62**: 140-147
53 **Padhani AR**, Gapinski CJ, Macvicar DA, Parker GJ, Suckling J, Revell PB, Leach MO, Dearnaley DP, Husband JE. Dynamic contrast enhanced MRI of prostate cancer: correlation with morphology and tumour stage, histological grade and PSA. *Clin Radiol* 2000; **55**: 99-109
54 **Jackson AS**, Reinsberg SA, Sohaib SA, Charles-Edwards EM, Jhavar S, Christmas TJ, Thompson AC, Bailey MJ, Corbishley CM, Fisher C, Leach MO, Dearnaley DP. Dynamic contrast-enhanced MRI for prostate cancer localization. *Br J Radiol* 2009; **82**: 148-156
55 **Engelbrecht MR**, Huisman HJ, Laheij RJ, Jager GJ, van Leenders GJ, Hulsbergen-Van De Kaa CA, de la Rosette JJ, Blickman JG, Barentsz JO. Discrimination of prostate cancer from normal peripheral zone and central gland tissue by using dynamic contrast-enhanced MR imaging. *Radiology* 2003; **229**: 248-254
56 **Ogura K**, Maekawa S, Okubo K, Aoki Y, Okada T, Oda K, Watanabe Y, Tsukayama C, Arai Y. Dynamic endorectal magnetic resonance imaging for local staging and detection of neurovascular bundle involvement of prostate cancer: correlation with histopathologic results. *Urology* 2001; **57**: 721-726
57 **Ren J**, Huan Y, Wang H, Chang YJ, Zhao HT, Ge YL, Liu Y, Yang Y. Dynamic contrast-enhanced MRI of benign prostatic hyperplasia and prostatic carcinoma: correlation with angiogenesis. *Clin Radiol* 2008; **63**: 153-159
58 **Kurhanewicz J**, Vigneron DB, Hricak H, Parivar F, Nelson

SJ, Shinohara K, Carroll PR. Prostate cancer: metabolic response to cryosurgery as detected with 3D H-1 MR spectroscopic imaging. *Radiology* 1996; **200**: 489-496

59 **Kurhanewicz J**, Vigneron DB, Nelson SJ. Three-dimensional magnetic resonance spectroscopic imaging of brain and prostate cancer. *Neoplasia* 2000; **2**: 166-189

60 **Scheidler J**, Hricak H, Vigneron DB, Yu KK, Sokolov DL, Huang LR, Zaloudek CJ, Nelson SJ, Carroll PR, Kurhanewicz J. Prostate cancer: localization with three-dimensional proton MR spectroscopic imaging--clinicopathologic study. *Radiology* 1999; **213**: 473-480

61 **Yacoe ME**, Sommer G, Peehl D. In vitro proton spectroscopy of normal and abnormal prostate. *Magn Reson Med* 1991; **19**: 429-438

62 **Schick F**, Bongers H, Kurz S, Jung WI, Pfeffer M, Lutz O. Localized proton MR spectroscopy of citrate in vitro and of the human prostate in vivo at 1.5 T. *Magn Reson Med* 1993; **29**: 38-43

63 **Mountford C**, Lean C, Malycha P, Russell P. Proton spectroscopy provides accurate pathology on biopsy and in vivo. *J Magn Reson Imaging* 2006; **24**: 459-477

64 **Schulte RF**, Trabesinger AH, Boesiger P. Chemical-shift-selective filter for the in vivo detection of J-coupled metabolites at 3T. *Magn Reson Med* 2005; **53**: 275-281

65 **Swindle P**, McCredie S, Russell P, Himmelreich U, Khadra M, Lean C, Mountford C. Pathologic characterization of human prostate tissue with proton MR spectroscopy. *Radiology* 2003; **228**: 144-151

66 **Costello LC**, Franklin RB. Aconitase activity, citrate oxidation, and zinc inhibition in rat ventral prostate. *Enzyme* 1981; **26**: 281-287

67 **Kurhanewicz J**, Dahiya R, Macdonald JM, Chang LH, James TL, Narayan P. Citrate alterations in primary and metastatic human prostatic adenocarcinomas: 1H magnetic resonance spectroscopy and biochemical study. *Magn Reson Med* 1993; **29**: 149-157

68 **Mountford CE**, Doran S, Lean CL, Russell P. Proton MRS can determine the pathology of human cancers with a high level of accuracy. *Chem Rev* 2004; **104**: 3677-3704

69 **Daly PF**, Lyon RC, Faustino PJ, Cohen JS. Phospholipid metabolism in cancer cells monitored by 31P NMR spectroscopy. *J Biol Chem* 1987; **262**: 14875-14878

70 **Fütterer JJ**, Heijmink SW, Scheenen TW, Jager GJ, Hulsbergen-Van de Kaa CA, Witjes JA, Barentsz JO. Prostate cancer: local staging at 3-T endorectal MR imaging--early experience. *Radiology* 2006; **238**: 184-191

71 **Morakkabati-Spitz N**, Bastian PJ, Gieseke J, Träber F, Kuhl CK, Wattjes MP, Müller SC, Schild HH. MR imaging of the prostate at 3.0T with external phased array coil - preliminary results. *Eur J Med Res* 2008; **13**: 287-291

72 **Turkbey B**, Pinto PA, Mani H, Bernardo M, Pang Y, McKinney YL, Khurana K, Ravizzini GC, Albert PS, Merino MJ, Choyke PL. Prostate cancer: value of multiparametric MR imaging at 3 T for detection--histopathologic correlation. *Radiology* 2010; **255**: 89-99

73 **Kim CK**, Park BK, Han JJ, Kang TW, Lee HM. Diffusion-weighted imaging of the prostate at 3 T for differentiation of malignant and benign tissue in transition and peripheral zones: preliminary results. *J Comput Assist Tomogr* 2007; **31**: 449-454

74 **Kim CK**, Park BK, Park W, Kim SS. Prostate MR imaging at 3T using a phased-arrayed coil in predicting locally recurrent prostate cancer after radiation therapy: preliminary experience. *Abdom Imaging* 2010; **35**: 246-252

S- Editor Cheng JX **L- Editor** Webster JR **E- Editor** Zheng XM